JOURNAL OF MATERIALS SCIENCE 32 (1997) 2549–2557

Evaluation of the tensile and fatigue behaviour of a powder metallurgy beryllium/aluminium alloy

V. C. NARDONE, T. J. GAROSSHEN
United Technologies Research Center, E. Hartford, CT 06108, USA

The tensile and fatigue behaviour of a powder metallurgy beryllium/aluminium alloy produced by Brush Wellman (Albemet 562) is determined as a function of temperature. The material is shown to have very high stiffness/density compared with common structural materials and moderate strength up to 232 °C. The mechanical properties of the material do not vary significantly as a function of orientation for the extruded plate evaluated in this study. The stiffness of the material can be readily explained using standard composite theory, where the material is treated as a beryllium particle-reinforced aluminium matrix composite. To explain the observed strength levels, a combination of microstructural-based dislocation strengthening mechanisms is proposed to act in combination with continuum mechanics strengthening based on load transfer. Failure analysis reveals that the aluminium regions of the material fail in a ductile dimple fashion, while the beryllium regions exhibit a more brittle cleavage type failure. Fatigue failure was found to initiate at inclusions present in the material, but is still very high relative to conventional aluminium alloys.

1. Introduction

There continues to be a need for high performance–low density materials in aerospace applications. One class of material currently under development for such applications is the beryllium–aluminium alloys being marketed by Brush Wellman under the tradename Albemet®. The Albemet alloys consist of 30 to 60 wt % beryllium (Be) with the balance being aluminium (Al). Since Be is almost insoluble in Al, the Albemet alloys essentially consist of a bimetallic structure of pure Be particles contained within an Al matrix. The presence of the Al regions in the Albemet alloys results in substantially improved ductility and fabricability relative to pure Be. As a result, the Albemet materials can be considered for structural applications and can be formed using conventional metal working processes such as extrusion and rolling.

Papers have been published that report on the property levels that can be achieved in the Albemet alloys [1–3]. However, this prior work was done on Albemet alloys that utilized pure Al as the matrix. In this particular study, the experimental Albemet 562 alloy was selected for evaluation. The "5" in the alloy designation exists because the Al matrix contains magnesium (Mg) at similar levels to 5000 series Al alloys. The "62" refers to the weight per cent Be present in the alloy. The current work determines both the tensile and fatigue performance of Albemet 562 as a function of temperature. A microstructural and failure mode analysis accompanies the mechanical property testing in order to help establish the microstructure/property relationships that exist for this material.

2. Materials

The Albemet 562 alloy was received from Brush Wellman in the form of a 1.27 cm × 11.4 cm cross-section extruded plate. After extrusion, the material was given a stress relief heat treatment consisting of 513 °C for 2 h followed by air cooling. Optical micrographs of the extruded material are shown in Figs 1 and 2. The Be phase, which constitutes ~ 70% of the material by volume, appears dark in the micrographs. This Be volume fraction level results in a material density of 2.13 g cm^{-3}. The Al matrix contains 3 wt % Mg. The Mg was added to the alloy to result in solid solution strengthening of the Al regions of the alloy.

Several observations can be made regarding the material microstructure shown in Figs 1 and 2. First, the size of the Be particles present in the alloy varies from about 1–10 μm. The typical size of the Be particles was about 3 μm, while the typical interparticle spacing was about 1 μm. Note that similar sized Be regions tend to be clustered within discrete regions of the material microstructure. This occurs as a result of the material fabrication route. Specifically, Albemet 562 is a powder metallurgy based material with the powder being made by inert gas atomization. The larger powder particles have slower cooling rates and therefore result in larger Be dendrites (particles) during solidification. The discrete regions of constant size Be particles observed in the alloy result from this powder metallurgy precursor material. Evidence of the powder precursor can be seen in the low magnification material cross-section shown in Fig. 1.

The low magnification longitudinal section of the material shown in Fig. 2 shows evidence of banding.

0022–2461 © *1997 Chapman & Hall*

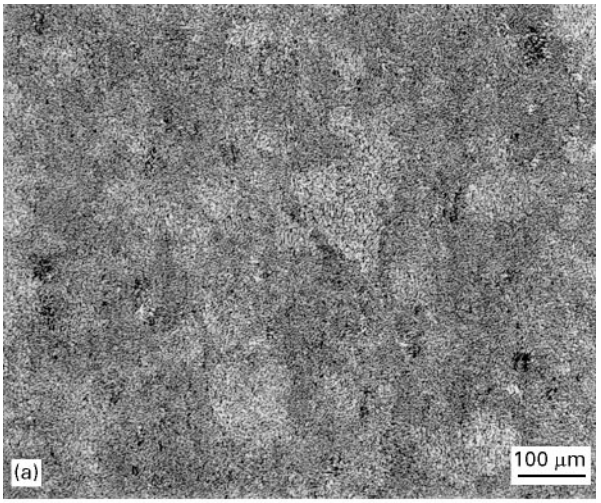

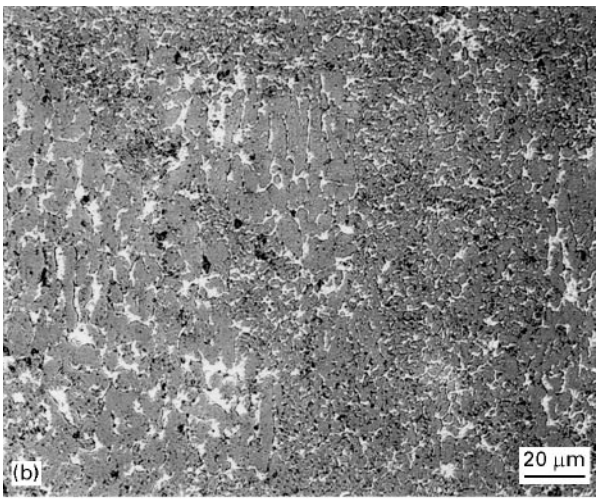

Figure 1 Cross-section of the Albemet 562 extruded plate.

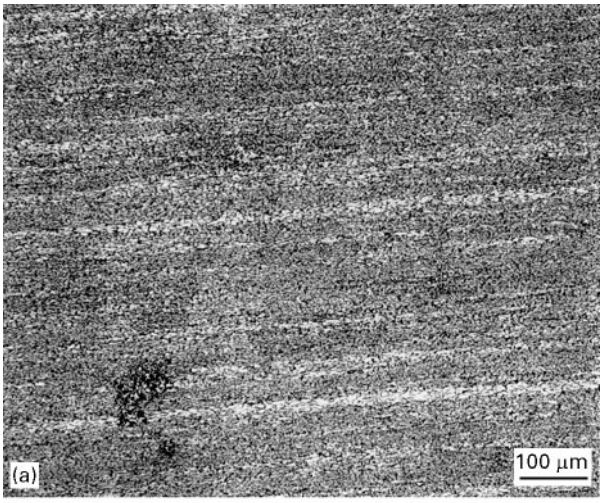

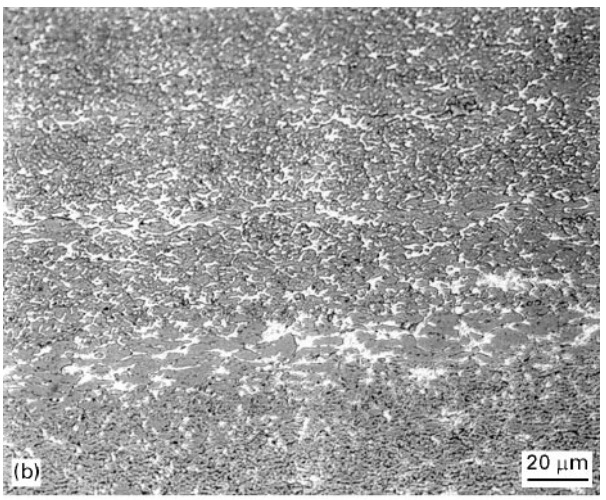

Figure 2 Longitudinal section of the Albemet 562 extruded plate.

The lighter banded regions correspond to the larger size powder particles that have become elongated during the extrusion process. The bands appear lighter because the material microstructure is more coarse in these regions. Although banding does exist, the higher magnification micrograph of Fig. 2 indicates that the individual Be particles do not have an appreciable aspect ratio.

3. Experimental procedure

Both tensile and fatigue properties were determined for the Albemet 562 alloy. The tensile testing was conducted at room temperature, 232 °C and 371 °C for both the longitudinal (parallel to the extrusion direction) and transverse (perpendicular to the extrusion direction) specimen orientations. The tensile tests were performed in triplicate with the average of the test values being reported. The tensile test specimen had a nominal 0.64 cm gauge diameter by 3.8 cm gauge length with threaded end attachment regions. The tensile testing was conducted at a constant cross-head displacement rate of 0.13 cm min^{-1}. Strain gauges bonded to opposite sides of the sample gauge region were used to measure the elastic modulus and 0.2% yield strength, while 2.54 cm gauge length extensometry was used to measure the sample failure strain.

All of the fatigue testing was conducted at 232 °C and an R value (ratio of minimum to maximum stress) of 0.1. A smooth cylindrical dogbone sample having a minimum diameter of 0.46 cm with threaded end regions was used for the fatigue testing. The testing was performed at frequencies ranging from 5 to 20 Hz, where the higher frequencies were used at the lower load levels.

Scanning electron microscopy (SEM) was performed on representative failed tensile and fatigue samples to assess the microstructural factors that influence material performance.

4. Experimental results

4.1. Tensile test results and failure analysis

A summary of the tensile test results is provided in Table I, while representative stress–strain curves as a function of temperature are shown in Figs 3 and 4. The results indicate that there is not a strong degree of anisotropy in the stiffness and strength of the material for testing in the longitudinal and transverse orientations. However, the transverse failure strains are about half that of the longitudinal values and the 371 °C transverse strength values are about 20% less than the longitudinal values.

TABLE I Tensile test results

Temperature (°C)	Elastic modulus (GPa)	Yield strength (MPa)	Tensile strength (MPa)	Failure strain (%)
Longitudinal orientation				
Room temperature	186	560	654	4.2
232	171	432	464	3.3
371	138	208	208	4.1
Transverse orientation				
Room temperature	191	531	618	2.3
232	182	427	465	0.9
371	140	165	178	1.7

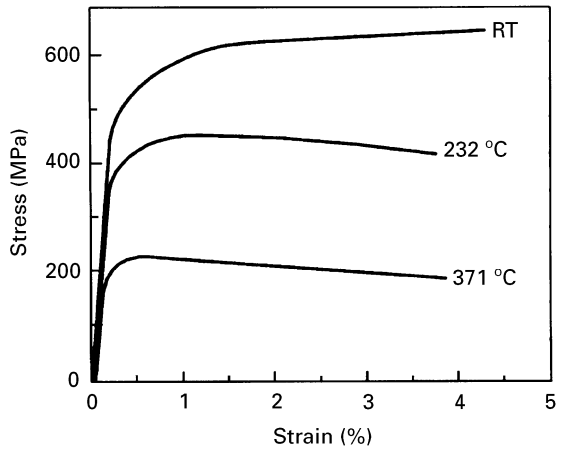

Figure 3 Longitudinal stress–strain curves as a function of temperature.

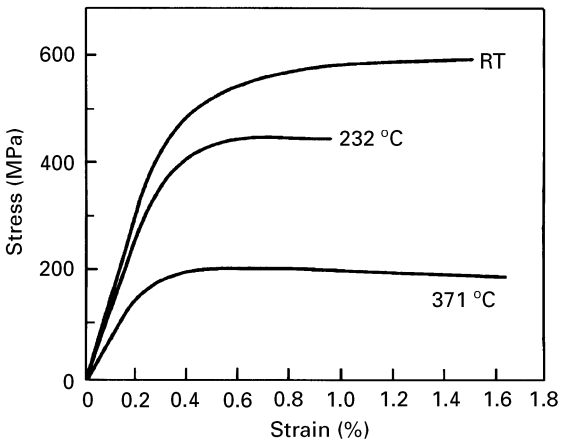

Figure 4 Transverse stress–strain curves as a function of temperature.

A comparison of the tensile fracture surface as a function of test orientation and temperature is shown in Figs 5 through 10. The room temperature and 232 °C fracture surfaces show similar features, while differences are apparent for the 371 °C samples. The fracture surfaces shown in Figs 5 and 6 show that the lower temperature samples have a relatively planar fracture surface, while the 371 °C samples have a much more undulating morphology. This difference in fracture surface morphology is further illustrated by the longitudinal sections through the fracture surfaces shown in Figs 7 and 8. For the high magnification fracture surface SEM micrographs shown in Figs 5, 6 and 9, all of the samples have similar features. Specifically, ductile dimple fracture of the Al regions is observed, while a cleavage type fracture is observed for the Be regions.

4.2. Fatigue test results and failure analysis

The results of the fatigue testing are summarized in Table II and Fig. 11. The data for both sample orientations appear to fall on a single fatigue curve. The resulting 232 °C 10^5 fatigue life is approximately 345 MPa, while the 10^7 fatigue life is about 241 MPa.

For all of the samples tested, failure initiated at an inclusion. A representative example of the fatigue fracture surface is shown in Fig. 12. In this case, the inclusion was about 100 μm in size and was Mg rich. The regions of the micrograph labelled 1, 2 and 3 roughly correspond to the crack initiation, crack growth and tensile overload regions of the fracture surface. Some crack growth was also detected in region 1 as labelled in Fig. 12. The results indicate that crack initiation in the samples is controlled by the presence of inclusions in the material.

The presence of the inclusions on all fatigue fracture surfaces prompted a more detailed evaluation of the inclusion content of the material. The inclusions were found to be magnesium oxides, which could also contain small amounts of Al, Si and Ca. The typical size of the inclusions was from 100 to 200 μm and the inclusion concentration was approximately 10 cm^{-2}.

5. Discussion

5.1. Material stiffness levels

Before proceeding into the analysis of the Albemet 562 stiffness levels, it is worth noting the unique stiffness to density ratio that this material possesses. The measured elastic modulus is about 188 GPa, which is similar to the value of steels and nickel base alloys. However, the density of the Albemet 562 is only 2.13 $g\,cm^{-3}$, which is about 20% lower than that of Al. From a stiffness/density ratio basis, Albemet 562 is about a factor of 3.5 times higher than conventional metals such as steel, nickel, titanium and aluminium. This certainly suggests that the material is well suited for stiffness critical applications.

The data indicate that the room temperature elastic modulus of the Albemet 562 material was similar for both the longitudinal and transverse orientations. Note that Albemet 562 essentially consists of pure Be particles that are embedded within an Al–Mg matrix. Therefore, one can analyse the properties of the material by treating it as a particle reinforced metal. The modulus of a discontinuously reinforced material can be calculated using the following Tsai–Halpin equation [4]

$$E_c = E_m(1 + C_L n V_p)/(1 - n V_p) \quad (1)$$

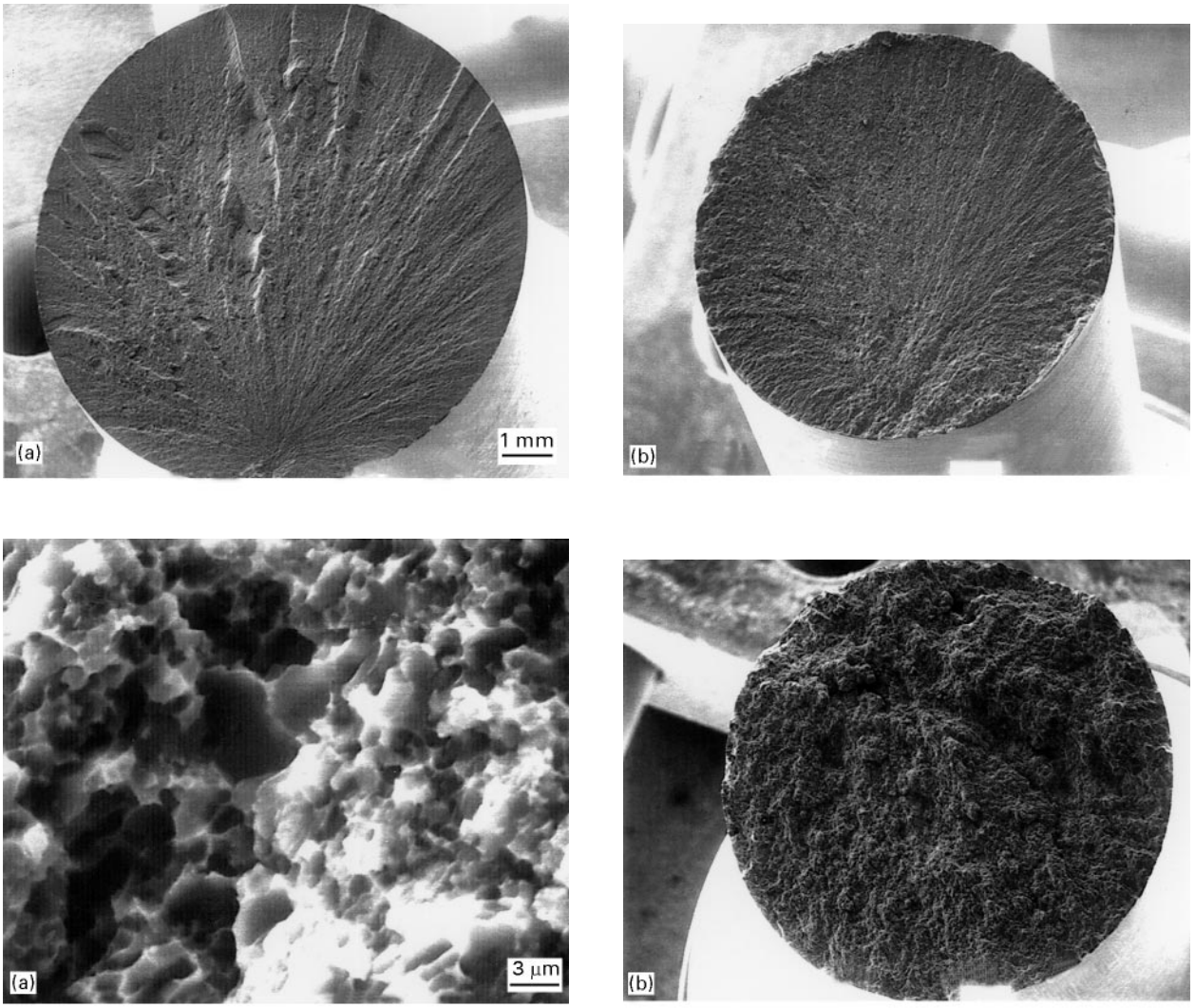

Figure 5 (a) SEM images of room temperature tensile fracture surface of a longitudinal sample. (b) SEM images of elevated temperature tensile fracture surfaces of longitudinal samples.

where E_c is the composite modulus, E_m is the matrix modulus and V_p is the reinforcement volume fraction. The value of n is equal to

$$n = (E_r/E_m - 1)/(E_r/E_m + C_L) \quad (2)$$

where E_r is the modulus of the reinforcement. Finally, the value of C_L is dependent on geometric factors, which for a particle reinforcement with limited aspect ratio is

$$C_L = 2 + 40V_p^{10} \quad (3)$$

The appropriate values for Albemet 562 are $E_m =$ 69 GPa (the modulus of Al), $E_r = 290$ GPa (the modulus of Be) and $V_p = 0.70$ (the volume fraction of Be).

Using the above equations and material constants, the calculated Albemet 562 material modulus is 193 GPa. The calculated modulus value is in excellent agreement with the experimentally measured numbers. This result indicates that the bond that exists between the Be and Al regions within the Albemet 562 is sufficient to permit effective load transfer from the Al to the stiffer Be. The net result is a material that behaves like a well-bonded particle reinforced metal–matrix composite.

The loss of modulus that occurs at elevated temperature in the Albemet 562 can be explained by the loss of modulus observed for monolithic Al and Be. Specifically, the modulus of Al–5%Mg at 371 °C has been reported to be about 52 GPa [5], while that of cross-rolled Be sheet has been reported to be about 248 GPa [6]. Substituting these elevated temperature modulus values for E_m and E_r result in a calculated value of $E_c = 159$ GPa. Here again, there is very good agreement between the calculated and the experimentally measured values. Thus, the good bonding between the Al and Be phases in the Albemet 562 material appears to be maintained at elevated temperature.

5.2. Yield strength levels

The room temperature yield strength of the Albemet 562 material is similar for both testing orientations, and is equal to about 545 MPa. This is a very high value considering the individual constituents that comprise the Albemet 562 material. The matrix is essentially an Al–3%Mg alloy, which is similar in composition to aluminium alloys 5052 and 5154. For alloys 5052 and 5154 Al, their yield strength is about

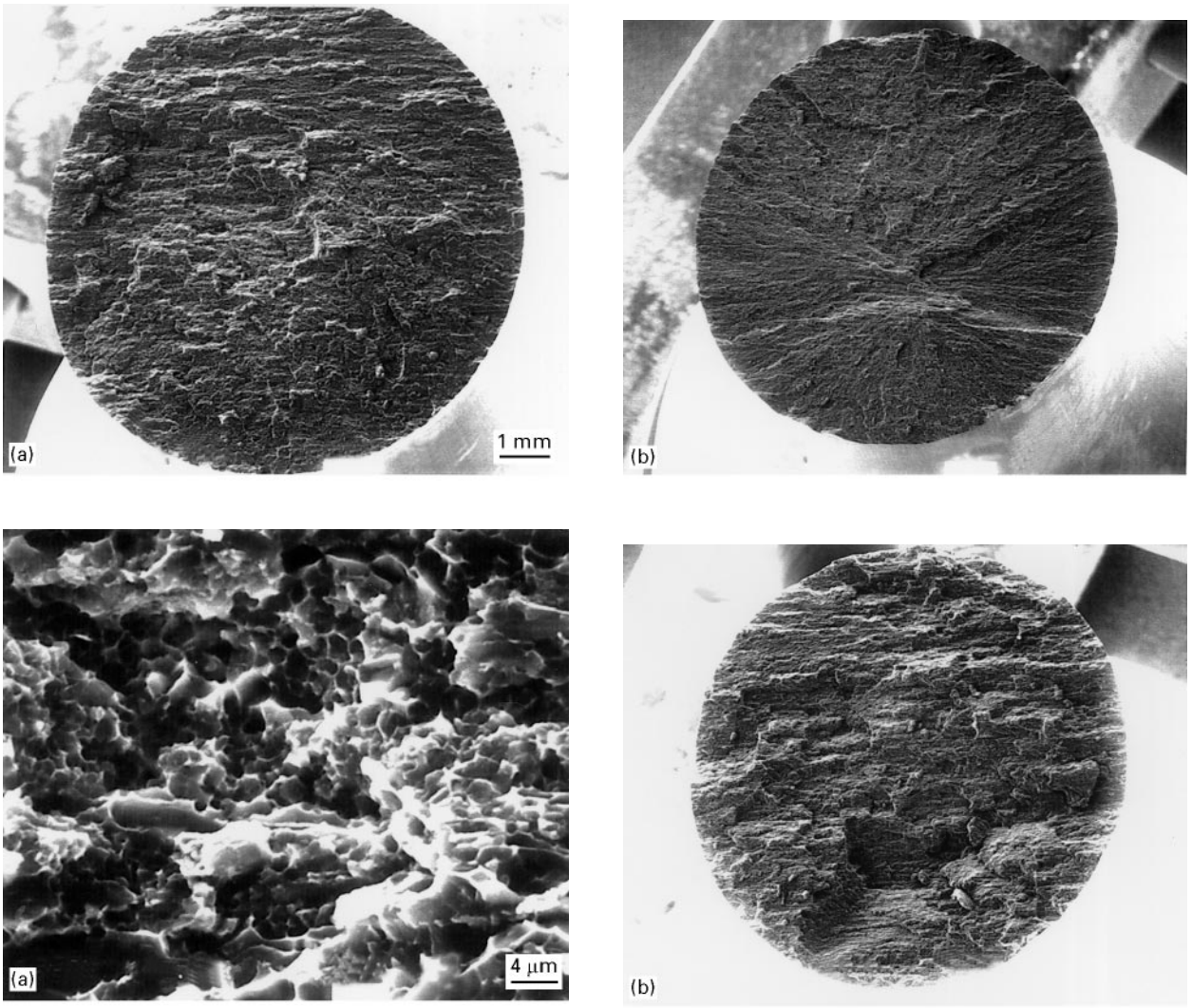

Figure 6 (a) SEM images of room temperature tensile fracture surface of a transverse sample. (b) SEM images of elevated temperature tensile fracture surfaces of transverse samples.

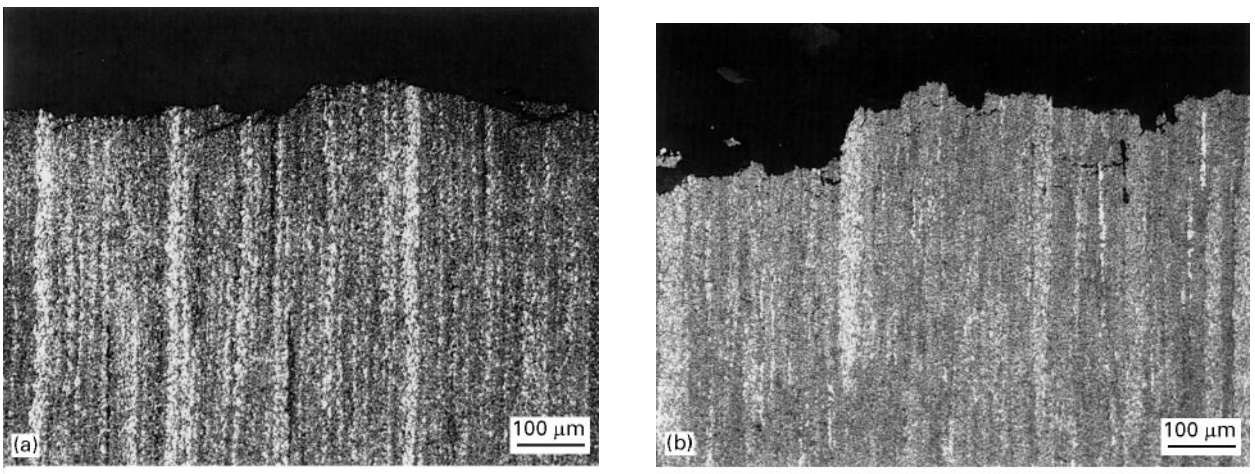

Figure 7 Longitudinal section through the tensile fracture surface of longitudinal samples. (a) Room temperature; (b) 371 °C.

103 MPa in the annealed condition and about 242 MPa in the strain hardened condition [7]. The strength values for Be vary significantly, depending on the product form. Yield strength levels of hot pressed block and cross-rolled sheet of various grades of Be are generally in the range of 210 to 415 MPa.

A reasonable question therefore arises concerning the operative strengthening mechanism in the Albemet 562 material. Strengthening mechanisms based on both dislocation micromechanics models and continuum models will be considered as discussed in detail below.

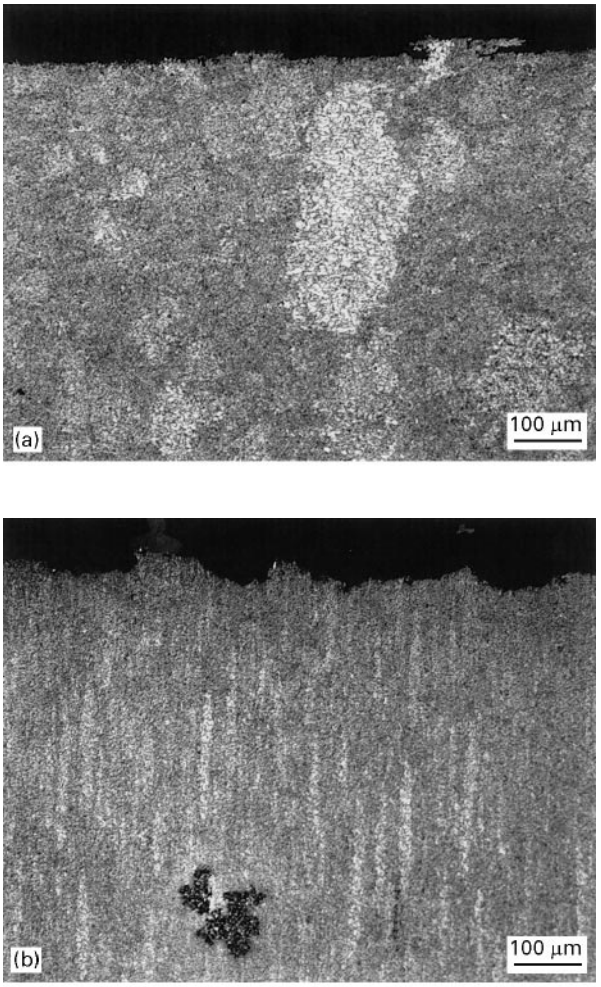

Figure 8 Longitudinal section through the tensile fracture surfaces of transverse samples. (a) Room temperature; (b) 371 °C.

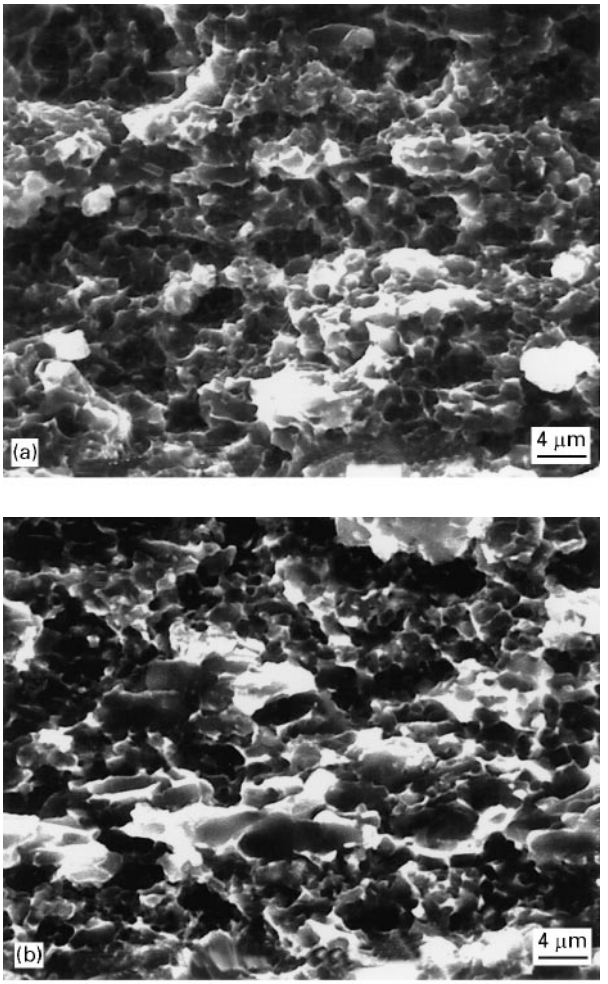

Figure 9 SEM images of tensile fracture surfaces of samples tested at 371 °C. (a) Longitudinal; (b) transverse.

5.3. Dislocation related strengthening mechanisms

Three distinct candidate strengthening mechanisms based on dislocation micromechanics will be considered, as previously done in the strength analysis of dispersion strengthened aluminium [8]: the Orowan mechanism, grain boundary strengthening (Hall–Petch strengthening) and an increase in dislocation density resulting from the relaxation of the thermal expansion mismatch between the Al and Be phases.

Before proceeding, it should be noted that the equations to be utilized here to estimate dislocation related strengthening increments are based on the assumption of uniform microstructural features. Clearly, the Albemet 562 material under consideration does not have a uniform microstructure. For the sake of the calculations, typical values will be used for the relevant microstructural dimensions. Therefore, the numerical results generated should be considered as a coarse estimate of the potential strengthening increments for each mechanism.

For the Orowan mechanism, the particle by-passing stress (τ_c) is predicted to be [9]

$$\tau_c = \frac{1.13Gb}{2\pi D} \ln (d/r_0) \quad (4)$$

where G is the matrix shear modulus (28 GPa), $\boldsymbol{b}$ is the Burger's vector (0.286 nm), d is the average Be particle size (3 μm), r_0 is the dislocation inner cut-off radius ($4\boldsymbol{b}$) and D is the average interparticle spacing (1 μm). The values utilized for d and D are typical values based on microstructural observations.

Substituting the above values into Equation 4 results in a calculated value for τ_c of 11 MPa. For a polycrystalline f.c.c. material, the projected yield strength increase from the Orowan mechanism is equal to $3\tau_c$ or 33 MPa. The result indicates that the Orowan mechanism can contribute slightly to the observed strength level of the Albemet 562 material, but is likely not the primary strengthening mechanism.

The second mechanism to be considered is the grain boundary strengthening mechanism. In this case, the strengthening increment (σ_{gb}) is calculated to be

$$\sigma_{gb} = KD_g^{-1/2} \quad (5)$$

where K is the Hall–Petch constant and D is the grain size. In this case, K will be taken to be 0.0725 MPa $m^{1/2}$ [8], while D_g will be assumed to be equal to the average interparticle spacing (1 μm). The calculated grain boundary strengthening increment is equal to 73 MPa or roughly twice that of the Orowan mechanism.

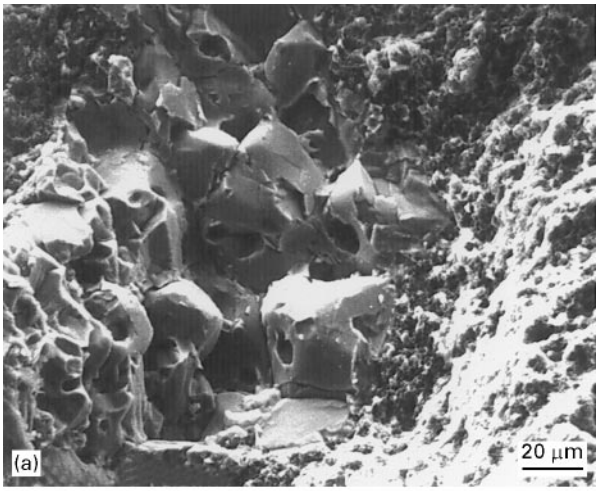

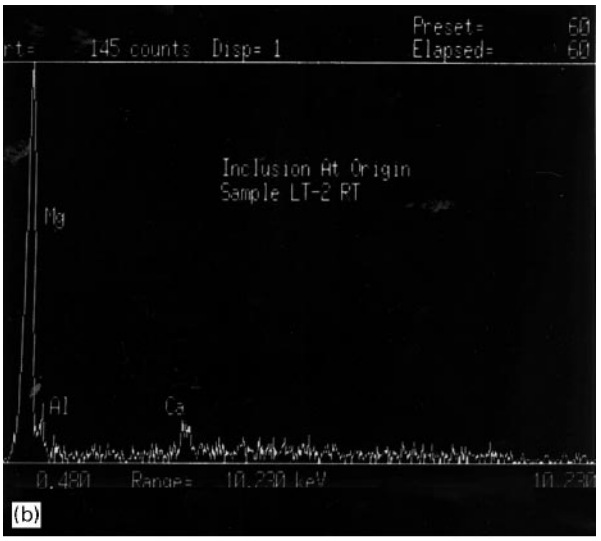

Figure 10 Fracture initiation site of a room temperature longitudinal tensile sample. (a) SEM; (b) EDS spectrum.

TABLE II Fatigue test results for testing at 232 °C and an R value of 0.1

Maximum stress (MPa)	Cycles to failure
Longitudinal orientation	
414	48 700
380	58 800
345	747 300
310	1 480 600
276	2 034 700
172	>10 000 000
Transverse orientation	
414	56 300
276	1 258 000
276	4 394 000
242	>10 000 000

Finally, the strengthening increment (σ_d) resulting from an increase in dislocation density owing to the relaxation of thermal expansion mismatch stresses is equal to [10]

$$\sigma_d = AG\boldsymbol{b}\rho_{th}^{1/2} \quad (6)$$

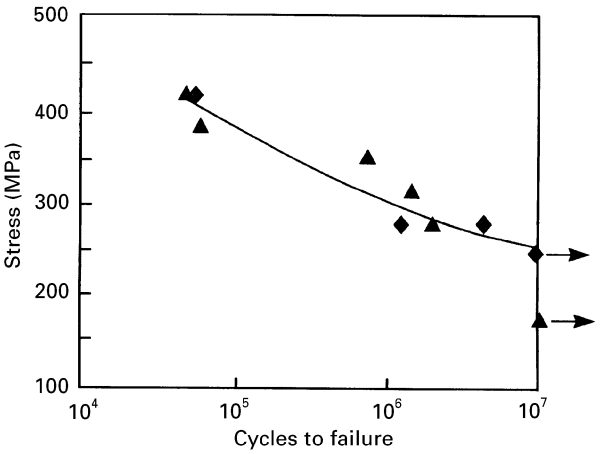

Figure 11 Fatigue data for the Albemet 562 material. (◆) Transverse; (△) longitudinal.

where A is a constant equal to 1.25 for aluminium [11] and ρ_{th} is the density of dislocation loops punched out by particles of diameter d. Assuming full relaxation of the mismatch owing to the difference of thermal expansion coefficients $\Delta\alpha$ for a temperature excursion ΔT [10]

$$\rho_{th} = \frac{12(2)^{1/2}\Delta\alpha\Delta T V_p}{\boldsymbol{b}d(1 - V_p)} \quad (7)$$

For Albemet 562 we assume that $\Delta\alpha$ is $3.6 \times 10^{-6}\,°C^{-1}$ and a value for ΔT of 250 °C [8]. Substituting the above values into Equations 6 and 7 results in a calculated value for σ_d of 65 MPa, which is similar to the calculated value for the Hall–Petch strengthening increment.

When the dislocation based strengthening mechanisms are looked at in total, it appears that the approximate strengthening increment is of the order of 175 MPa. The matrix in the annealed condition is anticipated to have a strength level of about 104 MPa as reported above. Note that the Albemet 562 material was annealed prior to testing. Thus, dislocation-based strengthening mechanisms would predict yield strength levels of the order of 276 MPa for the Albemet 562 material. In contrast, the measured yield strengths are about twice that value.

5.4. Continuum mechanics related strengthening

The very high stiffness levels measured in the Albemet 562 material indicate that load transfer in this system is effective. Therefore it is reasonable to consider whether load transfer from the Al to the Be can contribute to the observed strength level of the Albemet 562. For platelet reinforced composites, the predicted composite yield strength (σ_{cy}) is given by Nardone and Prewo's Equation 12 in [12]. For Albemet 562 it will be assumed that the particle aspect ratio is minimal, i.e. the particles are squares. Thus, $L_1 = L_2 = t$ of Nardone and Prewo's Equation 12 in [12] and the equation reduces to the following

$$\sigma_{cy} = \sigma_{my}[2V_p + (1 - V_p)] \quad (8)$$

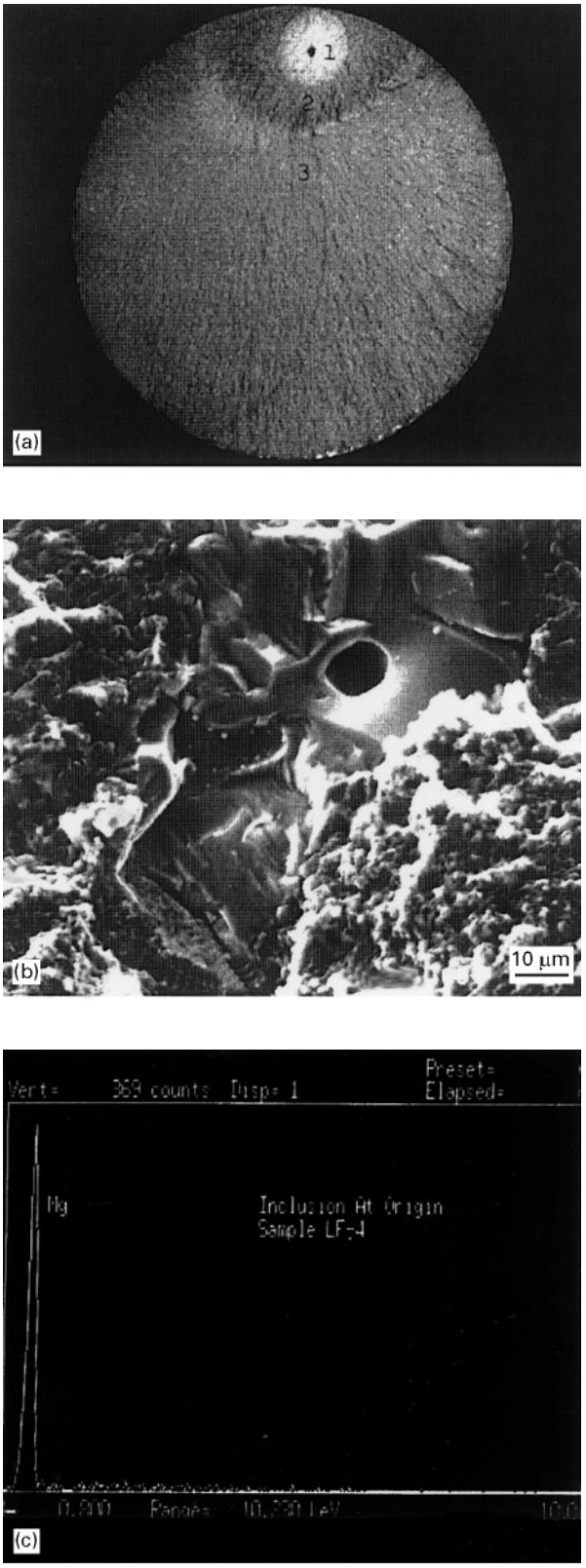

Figure 12 Fatigue fracture initiation site of a longitudinal sample: (a) optical micrograph; (b) SEM micrograph; (c) EDS spectrum.

where σ_{my} is the matrix yield strength. The value of V_p for Albemet 562 is 0.7, such that the calculated composite yield strength is equal to $1.7\sigma_{my}$. Note that this is a minimum expected contribution, since the aspect ratio of the Be particles in Albemet 562 is somewhat greater than 1.

The above result suggests that load transfer can play a very significant role in the observed strength level of Albemet 562. The appropriate value to use for σ_{my} would be the *in-situ* strength of the matrix within the composite, which based on the dislocation based strengthening mechanisms, is about 276 MPa. The net calculated material strength based on a superposition of dislocation and continuum based strengthening becomes 470 MPa which is reasonably close to the experimental value.

Another point worth noting with respect to the load transfer strengthening mechanism is the inherent assumption that the Be regions are sufficiently strong to sustain the transferred load without fracturing. Since the Be regions would bear a proportionally greater fraction of the applied load, the strength of these regions must be in excess of 690 MPa. Strength levels of 760 MPa have been reported for certain structural grades of extruded Be rod and tubing [6]. This suggests that strength levels of > 690 MPa for the very refined Be regions present in the Albemet 562 material are not unreasonable.

As mentioned above, precise agreement between the measured and calculated yield strength values would be fortuitous, because of the non-uniformity of the Albemet 562 microstructure. However, the calculations are very useful in terms of understanding the operative strengthening mechanisms. To summarize, it appears that dislocation-based strengthening mechanisms result in an increase in the *in-situ* strength of the Al within the Albemet 562 relative to what would be expected for the monolithic alloy. This strengthening increment while substantial, is not adequate to explain the observed Albemet 562 strength level. By recognizing that in addition to the dislocation-based strengthening there is a continuum load transfer strengthening effect operative as well, one can rationalize the observed yield strength of the Albemet 562 material. The decrease in strength as a function of temperature can simply be understood by recognizing the decrease in strength of the Al and Be regions with increasing temperature.

5.5. Description of the tensile sample failure models

The room temperature tensile fracture surface of the Albemet 562 material is planar in appearance (see low magnification photos of Fig. 5a for the longitudinal sample and Fig. 6a for the transverse sample). On a finer scale, the aluminium regions fail in a ductile dimple fashion while the Be phase fails in a more brittle cleavage mode (see high magnification photos in Figs 5a and 6a). The fracture appearance at 232 °C is similar to that observed at room temperature, while the 371 °C sample has a much more undulating topography (see Figs 5b and 6b). This latter feature can perhaps be more easily seen in the comparison of longitudinal sections through the fracture surfaces of samples shown in Figs 7 (longitudinal orientation) and 8 (tranverse). At high magnification, the 371 °C fracture surfaces (see Fig. 9) appear similar to that observed at room temperature (see Figs 5a and 6a).

One final observation should be noted concerning the failure analysis of the tensile samples. Inclusions were observed on about 30% of the samples tested.

One such inclusion may be observed in the optical micrograph longitudinal section of the sample shown in Fig. 8. A higher magnification SEM micrograph of the failure origin of the longitudinal room temperature sample shown in Fig. 5 is provided in Fig. 10. The origin contains a Mg-rich inclusion, with small amounts of Al and Ca, that was approximately 100 μm in size. However, the failure strain of the samples containing inclusions was similar to that of samples without inclusions on the fracture surface. This therefore suggests that the presence of an inclusion does not significantly effect the tensile properties of the material. A more detailed description of the inclusions is provided in Section 4.2.

5.6. Discussion of fatigue test results and failure analysis

The 10^7 fatigue runout stress of the Albemet 562 material for $R = 0.1$ testing at 232 °C is about 240 MPa. By way of comparison, the room temperature $R = 0.1$, 10^7 fatigue strength of hot-pressed Be block is about 240 MPa, while that of cross-rolled sheet is about 415 MPa. Thus, depending on processing conditions, Be can have reasonably high fatigue strength levels. For the Albemet 562, load transfer to the Be would likely lead to the fatigue strength of the composite being controlled by the fatigue strength of the Be regions. It is difficult to make an estimate of the inherent fatigue strength of the Be regions with Albemet 562, particularly at 232 °C. Note, however, in all cases fatigue was initiated at an inclusion. Thus the inherent fatigue strength of the Albemet 562 must be greater than the values measured in this study.

6. Summary

The Albemet 562 material is shown to have very high stiffness/density relative to common structural materials. Moderate strength levels are maintained at temperatures up to 232 °C, but fall off significantly at 371 °C. The mechanical properties of the material do not vary significantly as a function of orientation for the extruded plate evaluated in this study. Owing to the Be being insoluble in Al, discrete Be particles exist within the Al matrix of the alloy. The net result is the material behaving as a discontinuous Be particle-reinforced Al matrix composite. When the material is treated as a particle-reinforced composite, the measured stiffness levels can be readily explained using standard composite theory.

To explain the strength levels observed in the Albemet 562 material, a combination of microstructural-based dislocation strengthening mechanisms is proposed to act in combination with continuum mechanics strengthening based on load transfer. Specifically, calculations suggest that the refined microstructure present in the material result in significant grain boundary (Hall–Petch) strengthening and a strengthening increment (σ_d) resulting from an increase in dislocation density originating from the relaxation of thermal expansion mismatch stresses between the Be and Al phases. The net effect is a relatively strong *in-situ* Al matrix relative to what would be projected for a similar monolithic Al alloy. When the higher *in-situ* matrix strength is used in a model to predict the strength of discontinuously reinforced composites resulting from load transfer, the strength levels observed in Albemet 562 can be explained.

Finally, failure analysis reveals that the aluminium regions of the material fail in a ductile dimple fashion, while the beryllium regions exhibit a more brittle cleavage type failure. Fatigue failure was found to initiate at inclusions present in the material, but is still very high relative to conventional Al alloys.

Acknowledgements

The support of this work by the Office of Naval Research and the Naval Air Warfare Center is gratefully acknowledged. The programme was jointly monitored by Dr Steve Fishman and Dr Gil London and their technical guidance during the performance of this work is appreciated.

References

1. F. C. GRENSING and D. HASHIGUCHI, "Advances in Powder Metallurgy & Particulate Materials – 1995" (Metal Powder Industries Foundation, Princeton, NJ 1995) pp. 12–33.
2. D. HASHIGUCHI, A. N. ASHURST, F. C. GRENSING and J. M. MARDER, in Proceedings of the International Symposium on Advanced Materials for Lightweight Structures, ESTEC, Noordwijk, The Netherlands, 25–27 March, 1992 (ESA SP-336, October, 1992).
3. F. C. GRENSING and D. HASHIGUCHI, in "Advances in Powder and Particulate Materials", Vol. 4, (Metal Powder Industries Foundation, Princeton, NJ, 1993) pp. 179–89.
4. J. C. HALPIN, "Primer on composite materials: analysis", (Technomic Publishing Co., Lancaster, PA, 1984), p. 130.
5. R. F. WILDE and N. J. GRANT, *ASTM Proc.* **57** (1957) 917.
6. "Designing with beryllium", Brush Wellman Inc., Cleveland, OH.
7. J. A. NOCK Jr, in "Aluminium: Vol. I Properties, physical metallurgy and phase diagrams", edited by K. R. Van Horn, (American Society for Metals, Metals Park, OH, 1967) p. 314.
8. A. M. REDSTEN, E. M. KLIER, A. M. BROWN and D. C. DUNAND, *Mater. Sci. Eng.* **A201** (1995) 88.
9. M. F. ASHBY, "Physics of Strength and Plasticity", edited by M. F. Ashby and A. S. Argon, (Massachusetts Institute of Technology Press, Cambridge, MA, 1969) p. 113.
10. D. C. DUNAND and A. MORTENSEN, *Acta Metall. Mater.* **39** (1991) 127.
11. P. M. HAZZLEDINE, *Scripta. Metall. Mater.* **26** (1992) 57.
12. V. C. NARDONE and K. M. PREWO, *ibid.* **20** (1986) 43.

Received 11 July
and accepted 23 October 1996